Utilizing Boost and Double Injections for Enhanced Stratified-Charge DISI Operation with Gasoline and E30 Fuels

Wei Zeng, Magnus Sjöberg

Sandia National Laboratories. USA

E-mail: wei.g.zeng@gmail.com
Telephone: +(1) 9259803896
Fax: +(1) 9252941004

Abstract. This study systematically explores the effects of injection strategy and exhaust-gas recirculation (EGR) on boosted stratified-charge operation of a spark-ignition engine using gasoline and E30 fuels at absolute intake pressure from 100 kPa to 160 kPa. Nitrogen dilution is used to lower the intake mole fraction of oxygen to simulate the dilution effects of EGR. The engine is operated at 1000 rpm under part-load conditions with an $IMEP_g$ range of 380–680 kPa. For stratified operation with a single injection of gasoline, the application of intake boost lowers soot emissions substantially, but at the expense of decreased combustion stability and thermal efficiency. Fairly advanced injection and spark timings are required to avoid unstable combustion, but this leads to unfavorably advanced combustion phasing. Adding N_2 dilution slows combustion and retards combustion phasing such that a more thermodynamically favorable CA50 (5-8°CA ATDC) crank-angle range is achieved for $[O_2]$ in the range of 14% to 15%. The combination of N_2 dilution and CA50 retard reduces NO_x emissions strongly as a result of decreased peak combustion temperatures and shorter residence time at peak temperatures. However, combustion variability increases at low intake $[O_2]$. To restore combustion stability at high levels of simulated EGR, a double-injection strategy is applied. Systematic exploration of boosted stratified-charge operation with double injection reveals that a 70/30 split of total fuel mass with a 15°CA dwell between the start of injection events leads to stable combustion and low soot emissions, even at $[O_2]$ =14%.

High-speed flame natural luminosity imaging is conducted simultaneously through both a piston-bowl window and a side window to demonstrate the effect of double injection on flame propagation for stratified operation with low NO_x emissions at high EGR level. Heat-release rate based conditional analysis of the flame images shows that compared to a single-injection, double-injections creates a spark plasma that is more stretched out, correlating with a more stable early combustion. The conditional analysis of the flame images also demonstrates that double injection produces a more symmetric flame propagation with much smaller soot-containing regions, indicating a more favorable fuel distribution.

All-metal engine operation with gasoline and E30 fuels demonstrates similar engine performance and emission levels for boosted stratified operation with double injections. These observations suggest that E0 (gasoline)–E30 fuel blends can be compatible with highly efficient stratified-charge spark-ignited operation. However, for a 50/50 double-injection strategy, E30 showed elevated smoke emissions for operation without intake boost, indicating that certain operating strategies can be adversely affected by the ethanol content of E30 fuel blends.

In summary, a significant reduction of engine-out NO_x and soot emissions as well as stable combustion and high thermal efficiency can be achieved with a stratified-charge DISI engine when moderate to high levels of EGR are combined with a low boost level (absolute intake pressure 130 kPa) and a well-designed double-injection strategy.

1. Introduction

Increased engine efficiency is essential for complying with ever stringent fuel-economy standards (Federal Register 2012). Compared to conventional homogeneous charge direct-injection or port-fuel injected SI engines, the un-throttled stratified-charge (SC) direct-injection spark-ignited (DISI) engine has the potential for significantly improved thermal efficiency during part-load operation due to reduced pumping loss and overall lean operation (Sjöberg et al. 2014).

New-generation SC DISI engines, commonly referred to as spray-guided (SG) SC DISI engines, reached production in Europe initially in 2006 and continue in naturally aspirated and turbo-

charged designs (Altenschmidt et al. 2006, Fischer et al. 2006, Langen et al. 2007, Waltner et al. 2010, Lückert et al. 2011). Spray-guided combustion provides improved fuel economy and lower emissions as compared to traditional wall/air guided SC combustion system. The closely coupled injection and ignition and the carefully optimized piston bowl for these SG SC engines improve fuel economy by enabling stratified operation over larger ranges of speed, load, and charge dilution (Fansler et al. 2015). However, the close coupling of injection and ignition subjects the developing flame to high velocities and intense turbulence. The spark plasma, the ignition kernel and the developing flame all are subjected to steep and varying gradients in the liquid and vapor concentrations and the velocity fields (Peterson et al. 2011, Peterson et al. 2014, Fansler et al. 2002, Fansler et al. 2006, Fansler et al. 2008, Dahms et al. 2009, Dahms et al. 2011). These factors can produce unfavorable conditions during ignition and early flame-kernel growth, thus increasing the frequency of partial-burn and misfire cycles and decreasing combustion efficiency. Furthermore, high levels of exhaust-gas recirculation, whether by internal or external, are often used to reduce the oxygen concentration and increase the specific heat capacity of the charge, thereby leading to a decrease in the peak cylinder pressure and temperature and a reduction in NO_x emissions, but at the expenses of increased exhaust particulates and reduced combustion stability. Finally, SG SC DISI engines tend to have an overly advanced combustion phasing as a result of the closely coupled injection and ignition and the inability to retard the start of injection sufficiently due to subsequent fuel impingement on the piston bowl and insufficient fuel/air mixing. The 50% burn point (CA50) may even occur before top dead center (TDC) (Sjöberg and Reuss 2012, Sjöberg et al. 2014, Zeng et al. 2014). This leads to a reduction in thermal efficiency and promotes an increase in the formation of NO_x emissions due to a combination of higher in-cylinder gas temperature and longer residence time before expansion cooling.

The use of closely-spaced double injections is one potential solution to mitigate these constraints that inhibit widespread implementation of SG SC DISI engine (Schmidt et al. 2011). Advanced double-injection strategies have the potential to improve the mixture formation process, thereby enhancing the combustion stability. The use of two shorter injections may provide an opportunity to retard combustion phasing (CA50) to the thermodynamic optimum while achieving less fuel impingement on piston-bowl surfaces. The resulting lower peak combustion temperature also leads to reduced NO_x emissions.

Moreover, downsized boosted spark-ignited (SI) engines offer better fuel economy than naturally aspirated SI engines with the same torque and power levels and thus have rapidly become a megatrend in the automotive industry (Turner et al. 2014). The use of stratified operation for boosted engines allows significant improvements of part-load thermal efficiency due to reduced pumping loss and overall lean operation, as mentioned above. In addition, as the engine is operated with load control via fuel quantity alone for stratified operation, a higher mass flow can be maintained through the turbocharger at part loads (Schmidt et al. 2011). This would improve transient response and maintain high turbocharger efficiency. Higher intake pressures at boosted operation also leads to higher ambient in-cylinder charge density and compressed-gas pressure as compared to stratified operation at atmospheric condition. Therefore, boosted stratified operation has the potential to significantly suppress soot emissions due to less fuel impingement on the piston bowl.

This study focuses on systematically exploring the roles of boost and double-injection for spray-guided stratified operation with EGR using all-metal engine operation. The target is to demonstrate the best trade-off between NO_x and soot emissions while maintaining stable stratified operation and high thermal efficiency. Optical engine operation with high-speed plasma and flame imaging is conducted to provide the understanding of how double injections can improve stratified operation. Furthermore, given the current trends of increased use of alternative fuels, it is of interest to study how these processes are affected by the fuel type. Therefore, this study uses both gasoline and E30 (70% gasoline and 30% ethanol by volume). E30 represents an intermediate gasoline-ethanol fuel blend, and with its high octane number it has been identified as a promising fuel candidate for highly boosted SI engines (Anderson et al. 2012, Leone et al. 2014).

2. Experimental Hardware and Methods

2.1 Single-cylinder engine and operating conditions

This single-cylinder four-valve research engine was operated either with an all-metal configuration for continuously fired performance testing, or with a geometrically identical optical configuration for skip-fired imaging studies. Engine specifications and operating conditions are given in Table 1. Figure 1 shows a cross section of the combustion chamber at top-dead-center (TDC) and setup for

high-speed flame-luminosity imaging. The piston has a moderately deep piston bowl (Fig. 1B) to aid fuel stratification. For optical operation, the engine was equipped with a Bowditch-piston mirror (Fig. 1G), a piston-bowl window (Fig. 1C) and a quartz window in the end of the pent-roof section (Fig. 1D). The piston-bowl rim has a cut-out (right side of Fig. 1A) for better optical access into the bowl via the pent-roof side window (Fig. 1D). Both quartz windows are flat on the combustion-chamber side. The piston window is concave on the crank-case side, thereby creating a negative lens for a larger field of view. One of the intake valves (the lower-right valve in Fig. 1K) is deactivated to increase in-cylinder swirl and tumble levels (see Table 1), providing repeatable flow patterns for combustion stabilization (Zeng et al. 2015, Zeng et al. 2016). The engine has a centrally located 8-hole fuel injector with a nominal included angle of 60°. The spark-plug gap is located 13 mm away from the injector tip. Similar to previous studies (Sjöberg and Reuss 2012, Zeng et al. 2015), the injector is oriented such that two of the liquid spray plumes straddle the spark-plug gap.

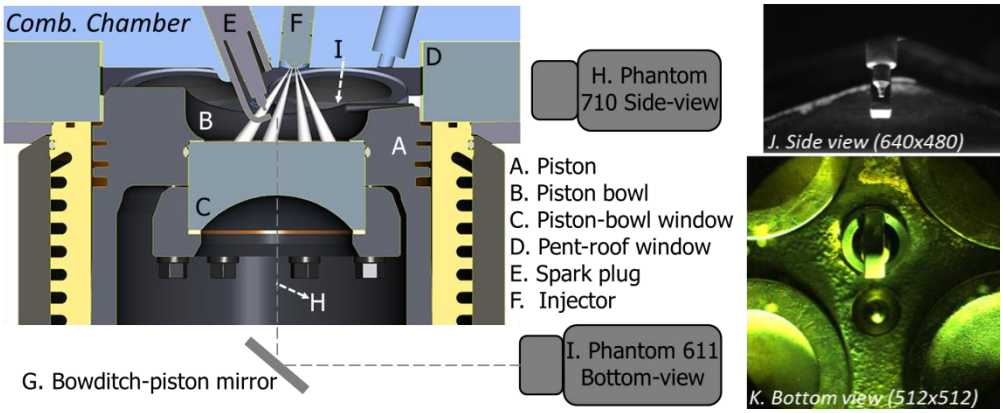

Fig. 1. Cross-section of combustion chamber at TDC and high-speed imaging setup with both side and bottom views obtained using high-speed monochrome (Phantom v710) and color cameras (Phantom v611), respectively

Table 1. Engine specifications and operating conditions

Bore/Stroke/ Displacement	86.0mm / 95.1mm / 0.55 liter				
Compression ratio / Engine speed	12:1/ 1000 rpm				
Ignition Energy / Duration	106 mJ / 1.0 ms				
Fuel injector	Bosch 8-hole VCO w/ 60° included angle				
Intake / coolant temperatures	25-28°C / 75 & 90°C				
Injection pressure (abs.)	17 MPa				
Injection strategy	Single, double				
Dwell between SOIs for double	15°CA				
Exhaust pressure (abs.)	100 kPa				
Swirl / Tumble index	2.7 / 0.6 (one intake valve deactivated)				
Intake [O_2] (simulated EGR w/ N_2)	14-19%				
Fuel	Gasoline			E30	
Intake pressure (abs., kPa)	100	130	160	100	130
Fuel per cycle (mg)	12.6	16.7	20.8	14.2	18.8
Combined gas (air+N_2) per cycle (g)	0.555	0.743	0.92	0.555	0.744
Gas (air+N_2)/fuel ratio	44.1	44.5	44.2	39.1	39.6

The effects of injection strategy and EGR on boosted stratified-charge operation are systematically studied using all-metal engine experiments with in-cylinder pressure and exhaust emissions measurements. For each operating point, the in-cylinder pressure is acquired for 500 consecutive cycles using 0.1°CA resolution with an uncooled Kistler 6125C piezoelectric sensor in combination with a Kistler 5010B charge amplifier. The variations of average indicated mean effective pressure – gross ($IMEP_g$) is less than 2% from day-to-day. To quantify combustion variability, the coefficient of variation (COV) of $IMEP_g$ is computed from all 500 cycles. The apparent heat-release rate (AHRR) is computed from the in-cylinder pressure for each individual cycle using a constant ratio of specific heats (γ=1.35) following (Heywood 1988). For computing combustion-phasing metrics like the 10% burn point (CA10), the AHRR is integrated over the crank-angle range for which AHRR is positive. A Horiba MEXA-584L emission analyzer measures CO, CO_2 and total HC. O_2 is measured with a CAI 600PP gas analyzer.

NO_x is measured with a CAI 600CLD gas analyzer. Exhaust smoke is measured with an AVL 415S smoke meter and reported as Filter Smoke Number (FSN). Exhaust smoke is also reported on a soot-mass basis, using the meter's internal correlation between paper blackening and soot concentration. The measured mole fractions of CO and HC are used to compute a metric of combustion efficiency. A complete description of the engine hardware and data acquisition can be found in previous papers (Sjöberg et al. 2014, Zeng et al. 2014, Sjöberg and Zeng 2016).

For all data in this study, the engine was operated in a manner that provides relatively low in-cylinder gas temperatures. First, the temperature of the fresh gases was close to room temperature (25–28°C). Second, the valve timings provide low residual levels (≈4-5% by mass) (Sjöberg et al. 2014). Third, a somewhat late intake valve closing makes the effective CR ≈ 11. Fourth, a coolant temperature of 75°C was selected for the all-metal tests. This lower-than-normal coolant temperature allows the use of elevated coolant temperature (90°C) for the skip-fired optical tests to achieve in-cylinder surface temperatures that are similar to those of the all-metal tests.

Stratified operation with gasoline and E30 fuels are compared. A certification gasoline with a high-octane value (AKI=92.7) was supplied by Haltermann Solutions as an exhaust-emissions and fuel-economy certification fuel for the US market and its specifications can be found in a previous paper (Dernotte et al. 2014). The E30 fuel was prepared in-house by blending the Haltermann certification gasoline with anhydrous high-purity ethanol in 70%/30% proportions by volume. Estimated properties of the E30 fuel are given in a previous paper (Sjöberg and Zeng 2016). For each intake pressure, the fuel mass per cycle is increased for E30 to compensate for its lower heating value as compared to gasoline.

2.2 Optical setup for high-speed flame natural luminosity imaging

High-speed flame natural luminosity imaging is conducted simultaneously with two cameras, providing both side (Fig. 1J) and bottom (Fig. 1K) views. This allows demonstrating the effect of injection strategy on flame propagation for stratified-charge operation. The optical setup is shown in Fig. 1. Images are recorded every 0.3°CA with two high-speed CMOS cameras, a Phantom v710 monochrome camera (Fig. 1H) and a Phantom v611 color camera (Fig. 1I). The monochrome camera is used with a 72 mm close-up lens to capture spark plasma and flame luminosity through the pent-roof window (Fig. 1D), providing an image resolution of 640×480 pixels. Simultaneously, the color camera is used with a lens of 180 mm focal length to record the combustion luminosity through the piston-bowl window (Fig. 1C), via a Bowditch-piston mirror (Fig. 1G), providing an image resolution of 512×512 pixels. The description of high-speed flame natural luminosity imaging with the v710 and v611 cameras can also be found in previous papers (Zeng et al. 2015, Zeng et al. 2016). The optical engine operates in a fire3-skip9 mode to reduce the thermal load on the quartz windows. All the data were acquired during the third fired cycle, which has residual gases that are representative of continuously fired operation with respect to temperature and composition.

3. Results and discussions

Here, only highly stratified operation (injection during the latter part of the compression stroke) is studied and nitrogen dilution is used to simulate EGR. Three intake pressures are used in this study: 100, 130 and 160 kPa absolute. The total gas charge mass is held constant at each intake pressure, while the intake oxygen mole fraction ($[O_2]$) is varied in a range of 14-19% to simulate various EGR levels. The exhaust pressure is held constant regardless of intake pressure. The fuel mass per cycle is increased with intake pressure to maintain a constant overall fuel/gas mass ratio, see Table 1.

In this study, the crank angles are referenced as after TDC of the combustion stroke, aTDC. For each injection, the start of injection (SOI) is the crank angle when the first liquid enters the combustion chamber, as determined by Mie-imaging via either the piston-bowl window or the pent-roof side window. Likewise, end of injection (EOI) is when the last liquid leaves the injector, as determined by Mie-imaging via the side window.

3.1 Boosted stratified operation with single-injection and EGR for gasoline

Figure 2 presents the combustion performance and instability as well as NO_x and soot emissions for boosted stratified operation with single-injection and EGR for gasoline. For stratified operation, the timing of the spark relative to that of fuel injection is important. A previous study (Sjöberg and

Reuss 2012) has demonstrated that a spark timing (ST) that closely coincides with EOI, igniting the tail of liquid spray, typically provides the most stable stratified operation for gasoline fuel. Because of this, the ignition-timing strategy dubbed "tail ignition (ST≈EOI)" is used for all stratified operation with gasoline in this paper. As noted in the legend of Fig. 2a, ST and EOI vary together with changes of the intake pressure such that the ST advance relative to EOI remains nearly constant.

A constant SOI of -31°CA aTDC is used to study the effect of N_2 dilution (simulated EGR) on stratified operation. This injection timing leads to an unfavorably early combustion phasing for $[O_2]$ = 16% - 19%, as shown in Fig. 2a. A combustion phasing that is thermodynamically more favorable can be achieved for these higher $[O_2]$ by retarding the injection timing, as the examples shown in Fig. 2b indicate. In this graph, $[O_2]$ = 16% for intake pressures of 100 kPa and 130 kPa. However, increased soot emissions and reduced combustion stability, perhaps due to fuel impingement on the piston bowl and insufficient fuel/air mixing, effectively prevent to use of SOI retard to achieve a thermodynamically favorable CA50 for stratified operation with single injection.

Figure 2a shows that a perhaps more viable option is to reduce $[O_2]$ further to 15% and 14%, whereby a thermodynamically favorable CA50 (5–10°CA aTDC) crank-angle range is achieved for each of the three intake pressures. Such reduction of $[O_2]$ reduces NO_x emissions strongly as well (Fig. 2d), as a result of decreased peak combustion temperatures and shorter residence time before expansion cooling. For such low $[O_2]$ operation, the $IMEP_g$ stability and soot emissions show a trade-off with the NO_x emissions, as shown in Fig. 2c and 2d. An examination of the EGR-induced trade-off between NO_x emissions and combustion stability for stratified operation has been discussed in Ref. (Sjöberg and Reuss 2012). Higher soot emissions at lower intake $[O_2]$ concentration can be anticipated due to an increase in both overall and local fuel/air ratios.

Compared to stratified combustion without boosting (100 kPa), boosted stratified operation (130 and 160 kPa) shows much lower soot emissions at all $[O_2]$ levels, as shown in Fig. 2d. However, Fig. 2c indicates that intake boost leads to elevated combustion variability for low intake $[O_2]$ concentrations of 14% and 15%. As mentioned above, the injection duration is adjusted to maintain a constant overall fuel/gas mass ratio regardless intake pressure. Therefore, the lower ISPM values for boosted operation are not caused by a reduction of the supplied fuel/air equivalence ratio (ϕ). A reduction of spray penetration and associated wall wetting as a result of higher in-cylinder gas density may be the primary reason for the strong reduction of soot emission when the intake pressure is increased from 100 to 130 kPa. Figure 2d also shows that the best trade-off between NO_x and soot emissions is achieved at an intake pressure of 130 kPa. For operation with an even higher intake pressure of 160 kPa, soot emissions rise. The cause of this is unclear, but it can be noted that CA50 is significantly more retarded for the 160 kPa case in comparison with the lower intake pressures (Fig. 2a). Therefore, an improvement of soot emissions at 160 kPa may be achieved by optimizing SOI and ST in future research. Here, the focus is on further improvement of the combustion stability at 130 kPa while maintaining low NO_x and soot emissions as well as favorable combustion phasing.

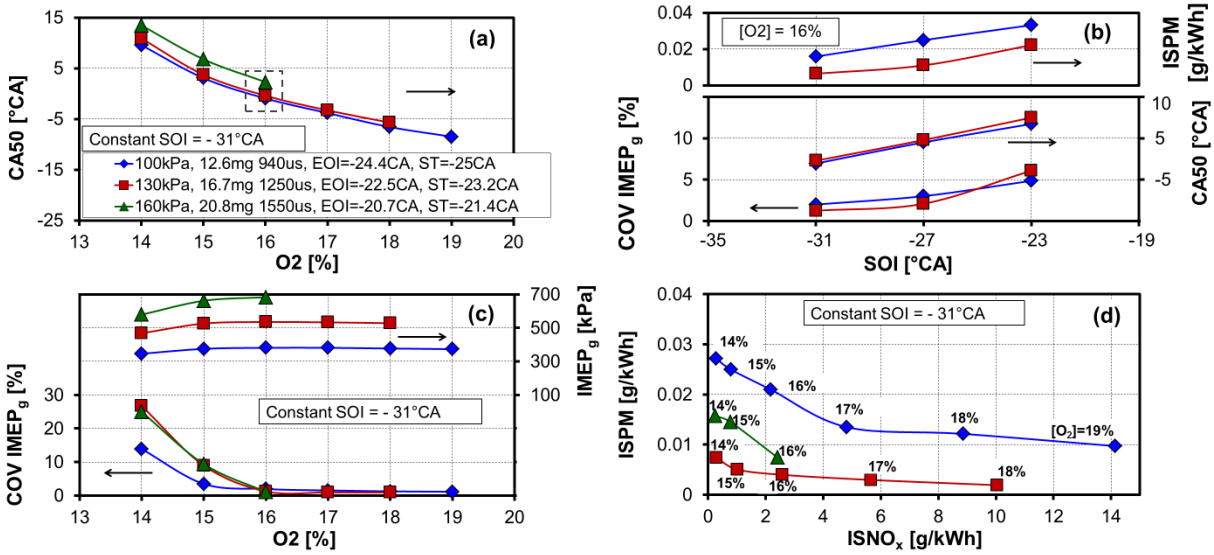

Fig. 2. a,c&d) Effect of EGR and intake pressure on CA50, $IMEP_g$, $IMEP_g$ instability, NO_x and soot emissions for stratified operation with gasoline and single-injection strategy. **b)** Effect of SOI retard for $[O_2]$ = 16%.

As discussed above, Fig. 2b demonstrates that it is not possible to use SOI retard for single-injection operation to achieve stable and low-soot operation with a favorable CA50. Therefore, a dou-

ble-injection strategy is proposed for this highly stratified operation to achieve further improvements of the NO_x / soot trade-off. In addition, closely coupled shorter injections could result in the formation of a stable charge mixture cloud in the spark-plug vicinity for an extended period of time (Schmidt et al. 2011). This has the potential to improve the trade-off between NO_x and combustion stability.

3.2 Role of double-injection for stratified operation with low NO_x emissions

All double-injection strategies in this study use SOI_1 = -40°CA aTDC for the first injection in combination with a constant dwell between start-of-injections (SOIs) of 15°CA, so that SOI of the second injection (SOI_2) = -25°CA. The selection of SOIs aims at (1) avoiding the formation of overly lean mixtures by the fuel injected in the first injection and (2) avoiding excessively late combustion phasing and severe wall wetting caused by the second injection. The dwell of 15°CA allows sufficient time for complete separation of the two injections such that the two injections do not interfere with each other. Two double-injection strategies are compared here: a 50/50 split with the same fuel mass per cycle for both injections, and 70/30 split with 70% fuel mass contributed by the first injection and the remainder by the second injection.

Results from an examination of viable ignition-timing strategies for stratified operation with a 50/50 split are shown in Fig. 3. It demonstrates that stable combustion can be accomplished by igniting either the first or the second spray. In either case, ST needs to coincide with the corresponding EOI to avoid misfires. This shows that the "tail ignition (ST ≈ EOI)" strategy provides the lowest combustion variability for stratified operation with double injections, in a similar manner to single injection operation. Igniting the first spray leads to higher combustion efficiency compared to igniting the second spray as earlier ST ensures that the majority of fuel/air mixture is consumed by the flame before it becomes overly lean. However, igniting the first spray significantly advances CA50 as compared to igniting the second spray, thus causing a reduced thermal efficiency. More importantly, igniting the first spray causes very high soot emissions (not plotted here) because the second spray then penetrates into already burning zones, as per the observations in Ref. (Genzale et al. 2011). Therefore, with the objective of improving NO_x / soot / stability trade-offs in the current research, a double-injection with ignition at EOI of the second spray (EOI_2) is used.

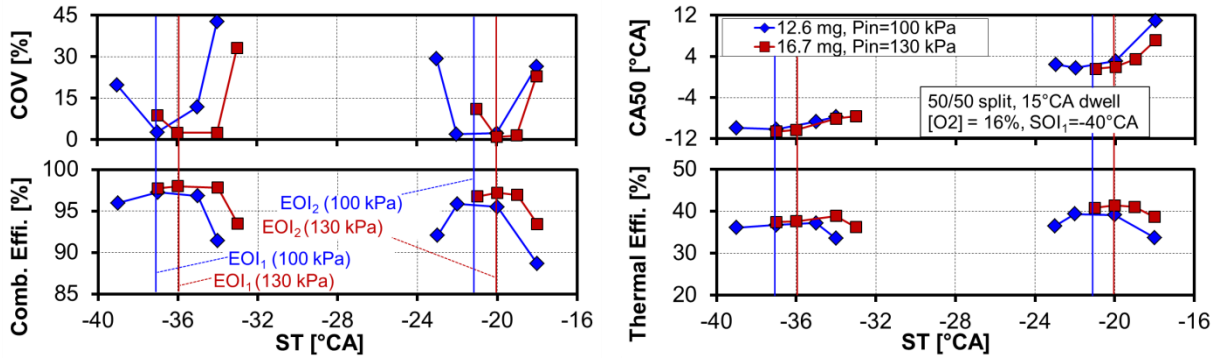

Fig. 3. ST sweep for double injections with 50/50 split using gasoline fuel and $[O_2]$ = 16%

Figure 4 compares the combustion performance and emissions for various injection strategies, spanning an intake $[O_2]$ range of 14%-16%. All conditions shown in Fig. 4 have 16.7 mg gasoline per cycle and an intake pressure of 130 kPa. As the "tail ignition" strategy is used for these operating conditions, ST relative to EOI_2 (or ST relative to EOI_1 for single injection) is used as x-coordinate for convenient comparison between various injection strategies. The EOI_2 (or EOI_1 for single injection) for each data set is listed in Fig. 4a.

Figure 4b shows that operation with double injection and a 50/50 split achieves stable operation (lowest COV of $IMEP_g$ < 3%) for both intake $[O_2]$ of 15% and 16%, while single injection cannot achieve stable combustion for $[O_2]$ = 15%. These results indicate that the use of double injections improves the dilution limit for stratified combustion. For operation with double injection and a 50/50 split, Fig. 4c shows that the combustion efficiency drops somewhat with a reduction of $[O_2]$ from 16% to 15%. However, the reduction of $[O_2]$ retards CA50 to a more favorable crank-angle range (Fig. 4d), which partly compensates for the combustion-efficiency loss. As a result, the $IMEP_g$ (Fig. 4a) level is similar for the two intake $[O_2]$ concentrations of 15% and 16%. Figures 4e and 4f demonstrate that for operation with double injection and a 50/50 split, reducing $[O_2]$ from 16% to 15% significantly suppresses NO_x emissions at the expense of elevated soot emissions. The higher exhaust soot level for

$[O_2]$ = 15% is consistent with an increase of the global fuel/air ratio, but it is not clear if increased soot formation or a deterioration of soot oxidation is the key factor.

Operation with $[O_2]$ = 15% and a 70/30 split results in a significant improvement of soot emissions compared to that of a 50/50 split, while maintaining low combustion variability and NO_x emissions. A reduction of wall wetting for the 70/30 split is a possible explanation for the reduction of soot emission. The amount of fuel mass injected by the second spray is reduced by 40%. In addition, the EOI_2 of the 70/30 split is slightly advanced in comparison with that of the 50/50 split due to a shorter injection duration of the second spray, as noted in the legend of Fig. 4a. The use of the 70/30 split significantly improves the trade-off between NO_x and soot emissions and between NO_x emissions and COV of $IMEP_g$ at $[O_2]$ = 15%. The 70/30 split allows extending the operating limit to $[O_2]$ =14% and achieving ultra-low NO_x emissions (43 ppm) with stable stratified operation (COV of $IMEP_g$ =2.2%).

Figure 5 summarizes the combined effects of double injections (70/30 split) and boost on stratified operation with EGR for gasoline. It can be concluded that a significant reduction in engine-out NO_x and soot emissions as well as stable combustion and high thermal efficiency can be achieved for a stratified-charge DISI engine when moderate to high level of EGR is combined with a low boost level (intake pressure = 130 kPa) and a well-designed double-injection strategy with a 70/30 split.

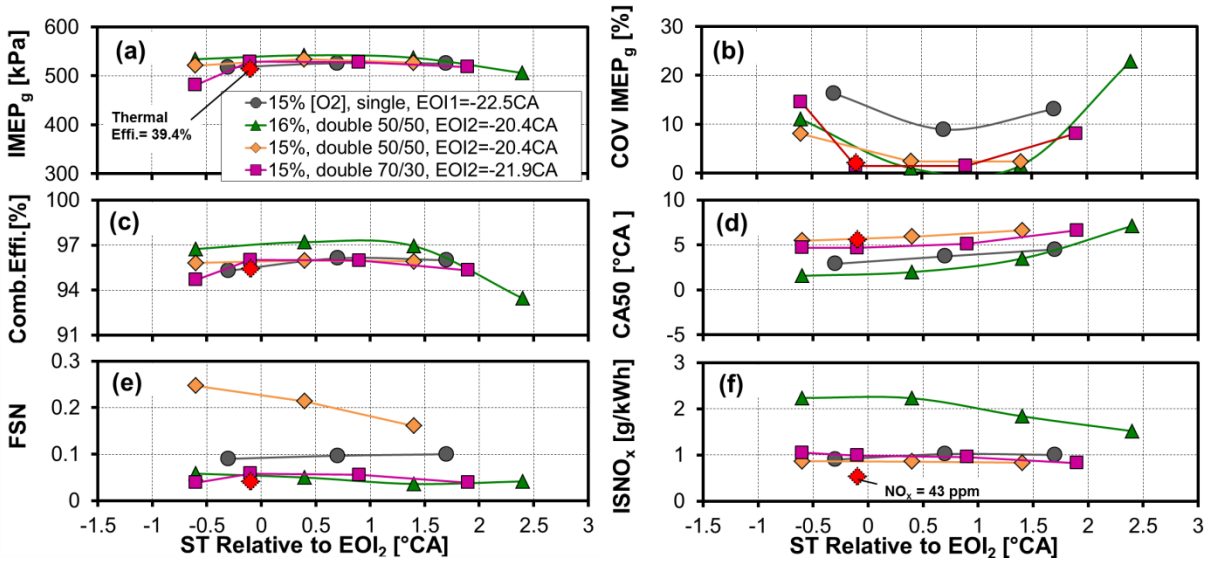

Fig. 4. $IMEP_g$, $IMEP_g$ variability, combustion efficiency, CA50, soot and NO_x emissions for various injection strategies at three intake $[O_2]$ concentrations for stratified operation with 16.7 mg gasoline at 130 kPa intake pressure. SOI = -31°CA for single injection. SOI_1 = -40°CA and SOI_2 = -25°CA for double injection.

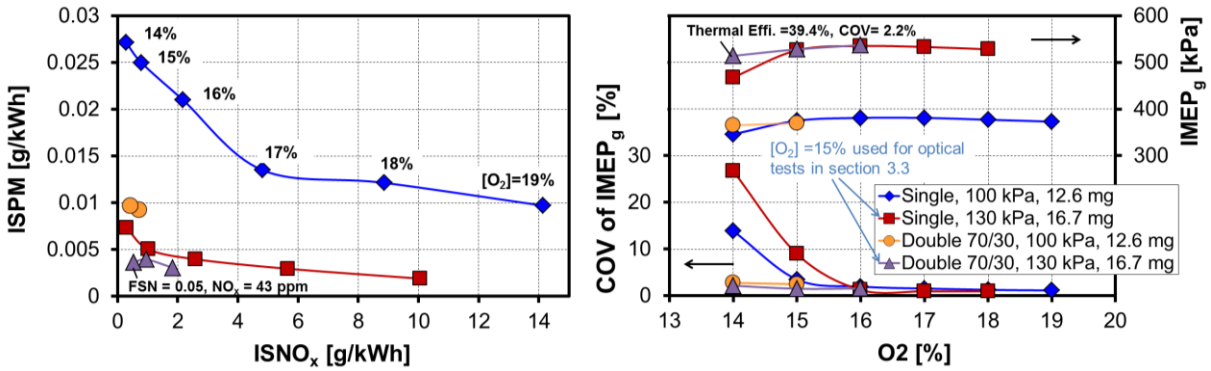

Fig. 5. The use of EGR, boost and double injections to achieve significant reductions of engine-out NO_x and soot emissions while maintaining low COV and high thermal efficiency for SC operation with gasoline.

3.3 Effect of double-injection on ignition and flame propagation for low-NO_x SC operation

The use of double injections allows the achievement of stable low-NO_x stratified-charge operation. Here, heat-release based conditional analysis of high-speed flame natural luminosity imaging is conducted to compare ignition and flame propagation for operation with single and double injections. The optical engine operation is focused on an intake pressure of 130 kPa with 16.7 mg gasoline at $[O_2]$

= 15%, as highlighted in Fig. 5. For the double injection operation, the 70/30 split with a dwell of 15°CA between SOIs is used and the SOI of the first spray (SOI_1) is -40°CA aTDC. The "tail ignition" ST strategy is also used for these optical operating conditions and the EOI and ST are indicated in Fig. 6a. Figure 6a presents ensemble-averaged apparent heat-release rate (AHRR) traces of both single- and double-injection conditions, indicating a slightly faster burn rate for operation with double injections. Operation with two injections also renders a smaller COV of $IMEP_g$, as noted in the text box of Fig. 6a. The IMEP variability of optical engine operation is in good agreement with that of all-metal operation (see Figs. 4b and 5).

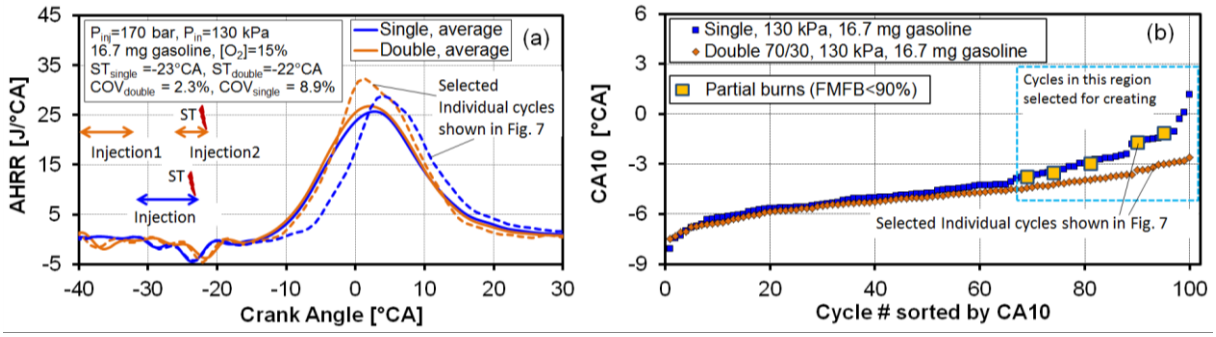

Fig. 6. (a) Average AHRR and statistically selected individual AHRR curves. (b) Cycle-to-cycle variations of CA10 and CA10 regions selected for producing flame probability maps for single- and double-injection conditions of optical engine operation.

Previous studies (Peterson et al 2014, Zeng et al. 2016) have revealed that the variability of ignition and early flame kernel growth contributes to the occurrence of partial-burn cycles for stratified combustion. Here, CA10 is chosen to be a representative marker of the early-burn timing. Figure 6b presents CA10 variations with cycle number sorted by CA10 and with the partial-burn cycles highlighted using larger squares. Following a previous study (Zeng et al. 2016), partial burns are defined to have a final mass fraction burned (FMFB) below 90%. 5 partial burns occur out of 100 cycles for single-injection operation, while all cycles for double-injection operation have a FMFB above 90%. Figure 6b indicates that there is a larger CA10 variability for operation with single injection and that all partial-burn cycles have a relatively late CA10. The most significant difference in CA10 variations between single- and double-injection is observed for cycles with relatively late CA10 where the CA10 curves separate, as highlighted using the dashed rectangle shown in Fig. 6b. Therefore, cycles in the dashed rectangle are selected to compare ignition and flame propagation for single- and double-injection operation.

Figure 7 presents flame images of statistically selected individual cycles (based on all cycles in the dashed rectangle) for both single- and double-injection operation. The AHRR traces are shown in Fig. 6a and the CA10 values are highlighted in Fig. 6b. A previous study (Zeng et al. 2016) compared the early flame kernel images of the natural luminosity captured with the Phantom v611 color camera to the OH* images captured with a high-speed intensified camera. This demonstrated that with a fully open aperture, the color camera is capable of detecting the weak early flame kernel. The luminosity from hot soot is significantly stronger than chemiluminescence emissions (such as OH* at 308 nm, CH* at 430 nm, etc.) of developing flame kernels. On the other hand, soot incandescence is primarily captured by red pixels of the color camera while the bluish chemiluminescence is primarily captured by the blue pixels. This allows the strong soot emissions to be suppressed to aid the presentation of the image data. Consequently, the RGB white-balance of all flame images presented here is altered from [1, 1, 1] to [0.6, 1, 1.8] to enhance the display of the weak early flames (see Fig. 7b at -13.5°CA), similar to the approach proposed in a previous paper (Zeng et al. 2016). Even so, the weak blue flame emissions mandate the use of a high image gain. As a result, the display of flames for mixing-controlled combustion of rich products tends to be saturated, despite the RGB adjustment, especially for bright soot luminosity. The image at 2.7°CA shown in Figure 7b is an example demonstrating both weak blue flame and bright soot luminosity.

All cycles in the dashed rectangle shown in Fig. 6b are used to produce probability maps to indicate the likelihood of flame location (shown in Fig. 8), following the approach discussed in a previous study (Zeng et al. 2011). The threshold value is chosen to be 100 out of a total image intensity depth of 4095. This threshold is based on empirical observation and makes the probability maps reflect the statistical location of both the weaker blue flame along with the higher intensity regions.

The images shown in Figs. 7 and 8 reveal that double injection creates a spark plasma that is more stretched out compared to single injection. The maximum plasma stretch is observed at the pre-

sented crank angle during spark discharge for each operating condition, -18.6°CA for single and -17.4°CA for double. Stretched plasma may indicate a favorable flow condition that can help combustion by moving the spark and early flame kernel away from the electrodes, a source of significant heat loss, and also by moving the kernel to a region of more favorable mixture fraction (Smith et al. 2011). More stretched plasma for double-injection agrees with a more stable early combustion (see Fig. 6b) as well as a larger and more consistent early flame kernel shown in Figs. 7 and 8 at -13.5°CA.

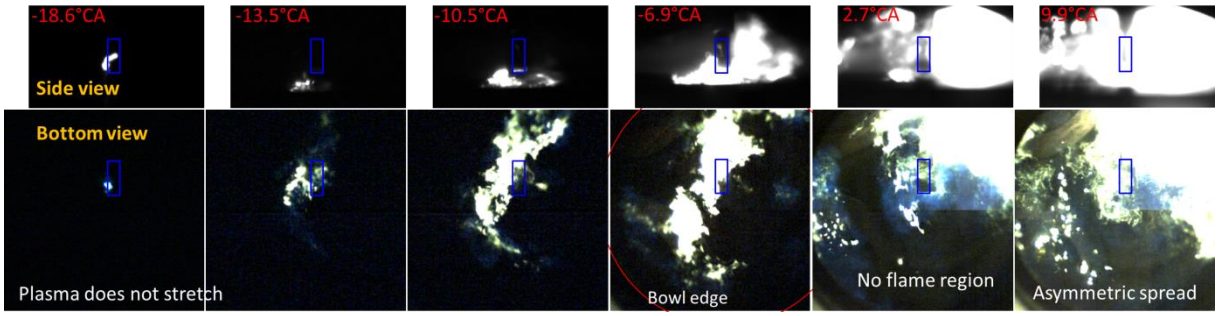

MFB<0.1% MFB<0.3% MFB<0.5% MFB=1% MFB=26% MFB=65%

(a) Single-injection

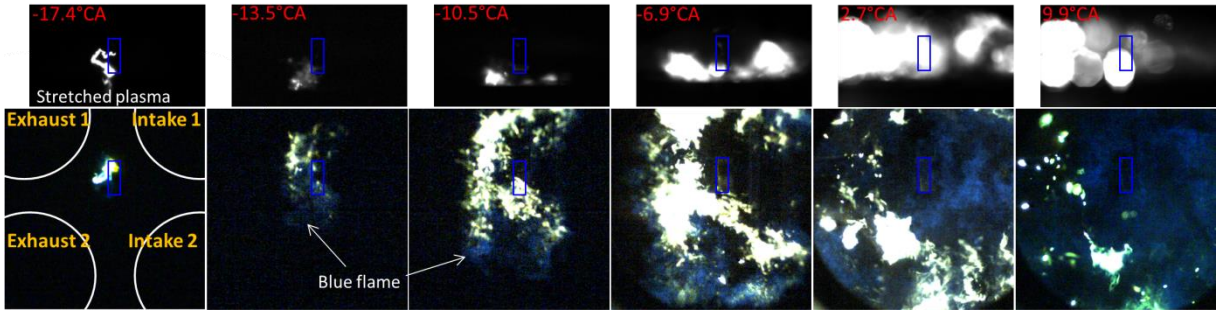

MFB<0.1% MFB<0.3% MFB<0.5% MFB=3% MFB=46% MFB=84%

(b) Double-injection

Fig. 7. Flame propagation of statistically selected individual cycle for (a) single- and (b) double-injection operation simultaneously imaged through side- and bottom-view. The spark plug location is indicated with blue rectangle.

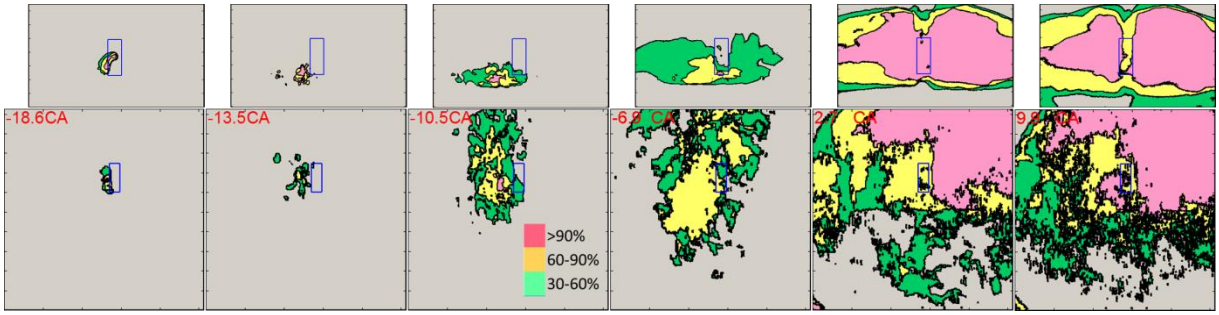

(a) Single-injection

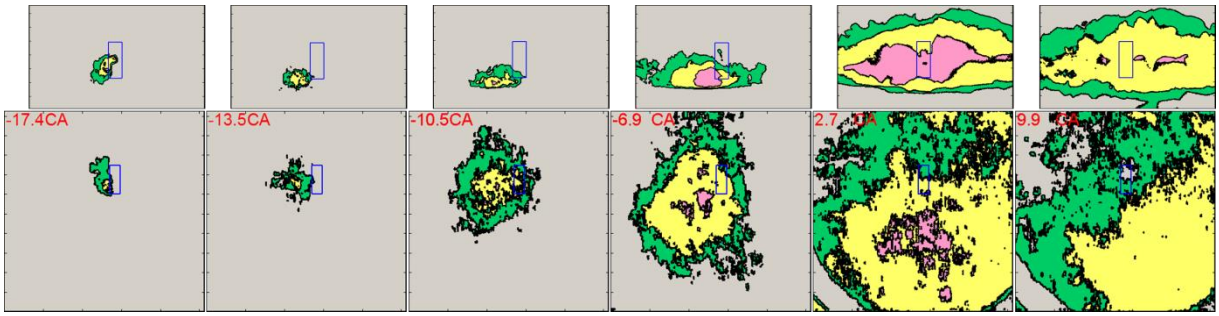

(b) Double-injection

Fig. 8. Flame probability maps for (a) single- and (b) double-injection operation using all cycles in the dashed rectangle shown in Fig. 6b.

Significant differences in flame pattern and intensity distributions between single- and double-injection are observed after spark discharge and early flame-kernel growth. Images at -10.5°CA and -6.9°CA show that flame propagation of these late-CA10 cycles with single injection tends to be less effective in the 6 o'clock direction, as viewed via the piston-bowl window (labeled "bottom view" in Figs. 7a and 1K). Later crank angles reveal inconsistent flame luminosity in the 4 to 8 o'clock directions, which is consistent with the low combustion efficiency indicated by FMFB < 90%. Furthermore, after TDC, the single injection generates larger areas with bright soot luminosity, and these are primarily located near intake valve #1 (valve labeling is defined in the -17.4°CA image of Fig. 7b).

In contrast, the double injection produces more symmetric flame propagation. Shortly after the spark discharge, the double injection displays flame propagation in both 12 and 6 o'clock directions, as seen in Fig. 7b at -10.5°CA and -6.9°CA. After TDC, flames fill the whole field of view in the piston bowl. It is also noteworthy that compared to single injection, the double injection produces a significantly smaller sooting flame region and more blue flame signal after TDC. Low-intensity blue flames consume large portions of the fuel during the latter part of the burn, indicating less fuel-rich combustion and more favorable mixture proportions and fuel distribution. The probability maps shown in Fig. 8 reflect these observations for individual cycles. It can be concluded that compared to double injection, the use of single injection causes a higher probability that the flame fails to propagate in the 4–8 o'clock direction, agreeing with the higher probability of the appearance of partial burns (FMFB<90%, see Fig. 6b). The likelihood for the double injection to create symmetric flame propagation is significantly higher than that of the single injection, corresponding to lower combustion variability.

Fig. 9 quantifies the difference in flame intensity between single- and double-injection. This average flame intensity is obtained first by spatially averaging the flame intensity for all red pixels of the color camera, and then ensemble averaging over all cycles highlighted in the dashed rectangle in Fig. 6b. Agreeing with the observation from the individual images shown in Fig. 7, double injection leads to significantly lower flame intensity compared to single injection because a significant amount of mixture is consumed by the low intensity blue flame for nearly every individual cycle with double injection. As highlighted in Fig. 9, the start of the first spray of double injection is earlier than the SOI of single injection. This illustrates that for double injection, the first spray has more time for fuel/air mixing, leading to a reduction of regions that are sufficiently rich to form soot. In addition, the amount of fuel supplied by the second spray that directly precedes ignition is much less than for the single-injection spray.

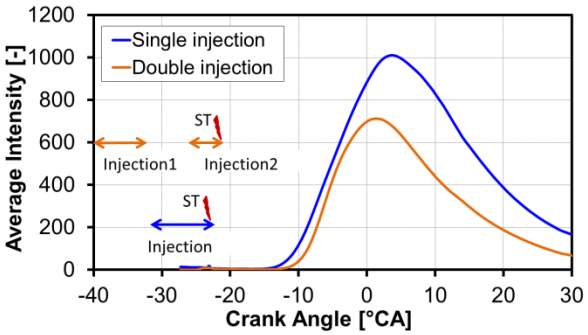

Fig. 9. Flame average intensity calculated using red pixels of color camera for single- and double-injection operation based on all cycles in the dashed rectangle shown in Fig. 6b.

3.4 Comparison of gasoline and E30 fuels for boosted stratified operation

In this work, the influence of fuel type on boosted stratified operation with double injections is initially examined for gasoline and a mid-level gasoline-ethanol fuel blend, E30, using all-metal engine experiments. The conditions used for comparison are the same to those shown in Fig. 3. A double-injection strategy with a 50/50 split and 15°CA dwell is used for stratified operation with gasoline and E30 fuels at two intake pressure levels, 100 kPa and 130 kPa. For each fuel, the fuel mass per cycle is increased at 130 kPa to maintain a constant ϕ = 0.43 at a fixed intake $[O_2]$ = 16%. For each intake pressure, injection duration is increased for E30 to compensate for its lower stoichiometric air/fuel ratio. Consistent with the approach used in section 3.3, here only spark timings near EOI of the second spray are examined. Constant SOI_1 = -40°CA and SOI_2 = -25°CA are used.

Figures 10a and 10b show that the spark-timing window with high $IMEP_g$ and low COV of $IMEP_g$ is roughly 1 to 2°CA wide for both gasoline and E30 fuels at either intake pressure. Figure 10a also shows that both gasoline and E30 fuels mandate a "tail-ignition strategy" with ST near EOI for

stable operation. In addition, Figs. 10b–10d demonstrate similar $IMEP_g$, combustion efficiency and CA50 for operation with gasoline and E30 fuels at either intake pressure. These results indicate that the difference in fuel properties between E30 and gasoline is sufficiently small so that combustion stability and performance remain similar for stratified operation with this double-injection strategy. Furthermore, Fig. 10f shows that the two fuels have similar NO_x emission level at either intake pressure.

However, Fig. 10e shows that at 100 kPa intake pressure, the use of E30 for the stratified operation with double injections leads to significantly higher soot emissions than for gasoline. It is hypothesized that the increased injection duration and stronger vaporization cooling of E30 could cause more severe wall wetting. Consistent with this hypothesis is the strong reduction of soot emission by the use of slight boost. Data at 130 kPa show that boosted stratified operation with both gasoline and E30 fuels achieve very low and comparable soot emissions. It is expected that higher ambient density at the boosted condition shortens liquid and vapor penetrations and strengthens flow-spray interaction, thus reducing wall wetting and improving fuel-air mixing. Even so, more research is required to understand the impact of mid-level ethanol on soot formation. Overall, the results for an intake pressure of 130 kPa in Fig. 10 suggest that E0 (gasoline)–E30 fuel blends can be made equally compatible with highly efficient boosted stratified-charge DISI operation.

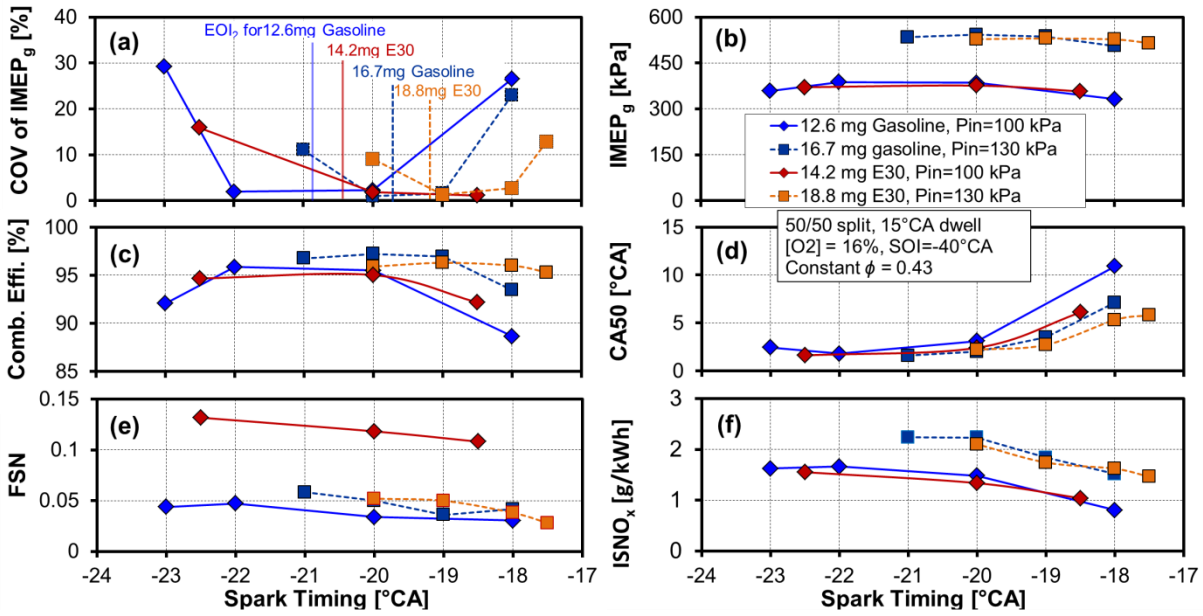

Fig. 10. Comparisons of combustion performance and emissions between gasoline and E30 fuels for stratified operation with double injections

4. Summary

This paper focuses on the use of intake boost and EGR for extending spray-guided stratified-charge DISI operation to higher loads at an engine speed of 1000 rpm. The use of single- and double-injection strategies for both naturally aspirated and boosted stratified-charge operation is compared for both gasoline and E30 fuels. Systematical all-metal engine experiments reveal that spray-guided stratified-charge operation at an $IMEP_g$ range of 380–530 kPa can achieve low soot (FSN < 0.05) and NO_x (≈43 ppm) emissions while maintaining low combustion variability (COV of IMEP < 2.5%) and high indicated thermal efficiency (≈40%). The key enabler is a well-designed double-injection strategy to improve combustion stability coupled with a high EGR level used to suppress NO_x emissions. For naturally aspirated operation using a highly diluted intake flow with $[O_2]$ = 14%, the double-injection strategy offers a much higher combustion stability with a COV of IMEP at 2.4%, as compared to a 15% COV of IMEP for the single-injection strategy. The use of the well-designed double-injection strategy also allows a significant reduction in engine-out soot emissions to a FSN value of 0.15, compared to a FSN value of 0.5 for the use of the single-injection strategy. Boosting the intake pressure from 100 kPa to 130 kPa allows reaching higher loads with further improved IMEP stability (2.2%) and reduced soot emissions (FSN = 0.05). All-metal engine operation with gasoline and E30 fuels demonstrates similar engine performance and emission levels for boosted stratified operation with double injections, indicating that E0 (gasoline) - E30 fuel blends can be made equally compatible with highly efficient

stratified-charge spark-ignited operation. However, E30 shows elevated soot emissions for naturally aspirated operation, perhaps due to stronger wall wetting of the piston bowl, indicating an area that needs to be addressed carefully in future research.

High-speed spark plasma and natural flame luminosity imaging reveal that stratified operation with double injection results in generally more stable combustion initiation and completion, as compared to single injection. In particular, double injection improves the early flame-kernel formation process by creating a spark plasma that is more stretched out, consistent with a more repeatable early flame propagation. Double injection also leads to a more symmetric flame propagation and higher combustion efficiency, indicating an improved fuel distribution. Finally, the imaging reveals a reduction of soot luminosity for double injection, suggesting a reduction of rich regions that form soot.

On a final note, these experiments utilize a strong swirl flow which is induced by deactivating one of the intake valves. Previous studies with a single injection have revealed that stratified operation with strong swirl leads to a more stabilized combustion due to reduced flow variations as a result of spray-swirl interaction (Zeng et al. 2015, Zeng et al. 2016). In the future, therefore, it is worthwhile to compare the role of single- and double-injection for spray-swirl interaction and reveal whether the double injection creates an even more stabilized flow compared to single injection.

Acknowledgments

The authors would like to thank Alberto Garcia, Gary Hubbard, Ken St. Hilaire, Keith Penney, Chris Carlen and Tim Gilbertson for their dedicated support of the DISI laboratory. Also, thanks to Dr. Ryan Gehmlich and Dr. David Vuilleumier for helpful discussions and for reviewing this paper.

This research was conducted as part of the Co-Optimization of Fuels & Engines (Co-Optima) project sponsored by the U.S. Department of Energy (DOE) Office of Energy Efficiency and Renewable Energy (EERE), Bioenergy Technologies and Vehicle Technologies Offices. Sandia is a multi-program laboratory operated by Sandia Corporation, a wholly owned subsidiary of Lockheed Martin Corporation, for the U.S. Department of Energy's National Nuclear Security Administration under contract DE-AC04-94AL85000.

Definitions/Abbreviations

ϕ	Fuel/Air Equivalence Ratio
°CA	Crank-Angle Degree
AHRR	Apparent Heat Release Rate
aTDC	after Top Dead Center
CA10	10% Burn Point
CA50	50% Burn Point
COV of IMEP	Coefficient of Variation of IMEP
DISI	Direct Injection Spark Ignition
E30	Blend of Gasoline with 30% Ethanol by Volume
EGR	Exhaust-Gas Recirculation
FSN	Filter Smoke Number
HC	(Unburned) Hydrocarbons
$IMEP_g$	Indicated Mean Effective Pressure – gross (2 strokes)
$ISNO_x$	Indicated Specific Nitrogen Oxides
ISPM	Indicated Specific Particulate Matter
MFB	Mass Fraction Burnt
NO_x	Nitrogen Oxides
SI	Spark Ignition
SOI	Start of Injection
EOI	End of Injection
ST	Spark Timing
TDC	Top Dead Center
VCO	Valve Covered Orifice

References

Altenschmidt F, Bertsch D and Bezner M (2006) The analysis of the ignition process on SI-engines with direct injection in stratified mode. Proceedings of the 7th International Symposium on Internal Combustion Diagnostics: Baden-Baden, Germany: pp 395-411.

Anderson J, DiCicco D, Ginder J, Kramer U, Leone T, Raney- Pablo H and Wallington T (2012) High octane number ethanol-gasoline blends: quantifying the potential benefits in the United States. Fuel: vol 97: pp 585-594.

Dahms RN, Fansler TD, Drake MC, Kuo TW, Lippert AM and Peters N (2009) Modeling ignition phenomena in spray-guided spark-ignited engines. Proceedings of the Combustion Institute: vol 32: pp 2743-2750.

Dahms RN, Drake MC, Fansler TD, Kuo TW and Peters N (2011) Understanding ignition processes in spray-guided gasoline engines using high-speed imaging and the extended spark-ignition model SparkCIMM. Part A: Spark channel processes and the turbulent flame front propagation. Combustion & Flame: vol 158: pp 2229-2244.

Dernotte J, Dec J and Ji C (2014) Investigation of the sources of combustion noise in HCCI engines, SAE International Journal of Engines: vol 7: pp 730-761.

Fansler TD, Stojkovic B, Drake MC and Rosalik ME (2002) Local fuel concentration measurements in internal combustion engines using spark-emission spectroscopy. Applied Physics B: vol 75: pp 577-590.

Fansler TD, Drake MC, Düwel L and Zimmermann FP (2006) Fuel-spray and spark plug interactions in spray-guided direct-injection gasoline engine. Proceedings of the 7th International Symposium on Internal Combustion Diagnostics: pp 81-97.

Fansler TD, Drake MC and Böhm B (2008) High-speed Mie-scattering diagnostics for spray-guided gasoline engine development. Proceedings of the 8th International Symposium on Internal Combustion Diagnostics: pp 413-425.

Fansler TD, Reuss DL, Sick V and Dahms D (2015) Combustion instability in spray-guided stratified-charge engines – a review. International Journal of Engine Research: vol 16: pp 260-305.

Federal Register (2012) Vol. 77, No. 199, 2017 and later model year light-duty vehicle greenhouse gas emissions and corporate average fuel economy standards.

Fischer J, Kern W and Unterweger G (2006) Methods for the development of the spray guided BMW DI combustion system. Proceedings of the 7th International Symposium on Internal Combustion Diagnostics: Baden-Baden, Germany: pp 413-423.

Genzale CL, Pickett LM, Hoops AA and Headrick JM (2011) Laser ignition of multi-injection gasoline sprays. SAE paper 2011-01-0659.

Heywood JB (1988) Internal Combustion Engine Fundamentals. McGraw-Hill, New York.

Langen P, Melcher T, Missy S, Schwarz C and Schünemann E. (2007) New BMW six- and four-cylinder petrol engines with high precision injection and stratified combustion. 28th International Vienna Motor Symposium.

Leone T, Olin E, Anderson J and Jung H (2014) Effects of fuel octane rating and ethanol content on knock, fuel economy, and CO_2 for a turbocharged DI engine. SAE International Journal of Fuels and Lubricants: vol 7: pp 9-28.

Lückert P, Breitbach H, Waltner A, Merdes N and Weller R (2011) Potential of spray-guided combustion systems in conjunction with downsizing concepts. 32nd International Vienna Motor Symposium.

Peterson B, Reuss DL and Sick V (2011) High-speed imaging analysis of misfires in a spray-guided direct injection engine. Proceedings of the Combustion Institute: vol 33: pp 3089-3096.

Peterson B, Reuss DL and Sick V (2014) On the ignition and flame development in a spray-guided direct-injection spark-ignition engine. Combustion & Flame: vol 161: pp 240-255.

Schmidt L, Seabrook J, Stokes J, Zuhdi MFA, Begg S, Heikal M and King J (2011) Multiple injection strategies for improved combustion stability under stratified part load conditions in a spray guided gasoline direct injection (SGDI) engine. SAE paper 2011-01-1228.

Smith J, Szekely G, Solomon A and Parrish S (2011) A comparison of spray-guided stratified-charge combustion performance with outwardly-opening piezo and multi-hole solenoid injectors. SAE paper 2011-01-1217.

Sjöberg M and Reuss D (2012) NO_X-reduction by injection-timing retard in a stratified-charge DISI engine using gasoline and E85. SAE International Journal of Fuels and Lubricants: vol 5: pp 1096-1113.

Sjöberg M, Zeng W and Reuss D (2014) Role of engine speed and in-cylinder flow field for stratified and well-mixed DISI engine combustion using E70. SAE International Journal of Engines: vol 7: pp 642-655.

Sjöberg M, Zeng W, Singleton D, Sanders JM and Gundersen MA (2014) Combined effects of multi-pulse transient plasma ignition and intake heating on lean limits of well-mixed E85 DISI engine operation. SAE International Journal of Engines: vol 7: pp 1781-1801.

Sjöberg M and Zeng W (2016) Combined effects of fuel and dilution type on efficiency gains of lean well-mixed DISI engine operation with enhanced ignition and intake heating. SAE Int. J. Engines vol 9(2): pp 750-767.

Turner JWG, Popplewell A, Patel R, Johnson TR, Darnton NJ, Richardson S, Bredda SW, Tudor RJ, Bithell CJ, Jackson R, Remmert SM, Cracknell RF, Fernandes JX, Lewis AGJ, Akehurst S, Brace CJ, Copeland C, Martinez-Botas R, Romagnoli A and Burluka AA (2014) Ultra boost for economy: extending the limits of extreme engine downsizing. SAE International Journal of Engines: vol 7(1): pp 387-417.

Waltner A, Lückert P, Doll G, Herwig H, Kemmler R and Weckenmann H (2010) The new V6 petrol engine with direct injection from Mercedes-Benz. 31st International Vienna Motor Symposium.

Zeng W, Sjöberg M and Reuss D (2014) Using PIV measurements to determine the role of the in-cylinder flow field for stratified DISI engine combustion. SAE International Journal of Engines: vol 7: pp 615-632.

Zeng W, Sjöberg M and Reuss DL (2015) PIV examination of spray-enhanced swirl flow for combustion stabilization in a spray-guided stratified-charge direct-injection spark-ignition engine. International Journal of Engine Research: vol 16: pp 306-322.

Zeng W, Sjöberg M, Reuss DL and Hu Z (2016) The role of spray-enhanced swirl flow for combustion stabilization in a stratified-charge DISI Engine. Combustion and Flame: vol 168: pp 166-185.

Zeng W, Sjöberg M, Reuss DL (2015) Combined effects of flow/spray interactions and EGR on combustion variability for a stratified DISI engine. Proceedings of the Combustion Institute: vol 35: pp 2907-2914.

Zeng W, Idicheria C, Fansler T and Drake M (2011) Conditional analysis of enhanced combustion luminosity imaging in a spray-guided gasoline engine with high residual fraction. SAE paper 2011-01-1281.